ESC European Society of Cardiology

European Heart Journal (2021) **42**, 4264–4276
doi:10.1093/eurheartj/ehab298

TRANSLATIONAL RESEARCH
Congenital heart disease

Endocardial/endothelial angiocrines regulate cardiomyocyte development and maturation and induce features of ventricular non-compaction

Siyeon Rhee[1†], David T. Paik[2,3,4†], Johnson Y. Yang[2,3,4], Danielle Nagelberg[1], Ian Williams[1,2], Lei Tian[2,3,4], Robert Roth[1], Mark Chandy[2,3,4], Jiyeon Ban[1], Nadjet Belbachir[2,3,4], Seokho Kim[5], Hao Zhang[2,3,4], Ragini Phansalkar[6], Ka Man Wong[1], Devin A. King[1], Caroline Valdez[1], Virginia D. Winn[7], Ashby J. Morrison[1]*, Joseph C. Wu[2,3,4]*, and Kristy Red-Horse[1,2,4]*

[1]Department of Biology, Stanford University, Stanford, CA 94305, USA; [2]Stanford Cardiovascular Institute, Stanford University School of Medicine, Stanford, CA 94305, USA; [3]Department of Medicine, Division of Cardiology, Stanford University School of Medicine, Stanford University, Stanford, CA, USA; [4]Institute for Stem Cell Biology and Regenerative Medicine, Stanford University School of Medicine, Stanford, CA 94305, USA; [5]Department of Developmental Biology, Stanford University School of Medicine, Stanford University, Stanford, CA 94305, USA; [6]Department of Genetics, Stanford University School of Medicine, Stanford University, Stanford, CA 94305, USA; and [7]Department of Obstetrics and Gynecology, Stanford University School of Medicine, Stanford University, Stanford, CA 94305, USA

Received 15 July 2020; revised 21 April 2021; editorial decision 27 April 2021; accepted 15 May 2021; online publish-ahead-of-print 19 July 2021

See page 4277 for the editorial comment for this article 'The endothelial niche in heart failure: from development to regeneration', by J.U.G. Wagner and S. Dimmeler, https://doi.org/10.1093/eurheartj/ehab304.

Aims Non-compaction cardiomyopathy is a devastating genetic disease caused by insufficient consolidation of ventricular wall muscle that can result in inadequate cardiac performance. Despite being the third most common cardiomyopathy, the mechanisms underlying the disease, including the cell types involved, are poorly understood. We have previously shown that endothelial cell-specific deletion of the chromatin remodeller gene *Ino80* results in defective coronary vessel development that leads to ventricular non-compaction in embryonic mouse hearts. We aimed to identify candidate angiocrines expressed by endocardial and endothelial cells (ECs) in wildtype and LVNC conditions in *Tie2Cre;Ino80$^{fl/fl}$* transgenic embryonic mouse hearts, and test the effect of these candidates on cardiomyocyte proliferation and maturation.

Methods and results We used single-cell RNA-sequencing to characterize endothelial and endocardial defects in *Ino80*-deficient hearts. We observed a pathological endocardial cell population in the non-compacted hearts and identified multiple dysregulated angiocrine factors that dramatically affected cardiomyocyte behaviour. We identified *Col15a1* as a coronary vessel-secreted angiocrine factor, downregulated by *Ino80*-deficiency, that functioned to promote cardiomyocyte proliferation. Furthermore, mutant endocardial and endothelial cells up-regulated expression of secreted factors, such as *Tgfbi, Igfbp3, Isg15*, and *Adm*, which decreased cardiomyocyte proliferation and increased maturation.

Conclusions These findings support a model where coronary endothelial cells normally promote myocardial compaction through secreted factors, but that endocardial and endothelial cells can secrete factors that contribute to non-compaction under pathological conditions.

* Corresponding authors. Tel: +(650) 721-6589, Email: ashbym@stanford.edu (A.J.M.); Tel: +(650) 736-2246, Email: joewu@stanford.edu (J.C.W.); Tel: +(650) 736-9506, Email: kredhors@stanford.edu (K.R.-H.)
† These authors contributed equally to this work.

Graphical Abstract

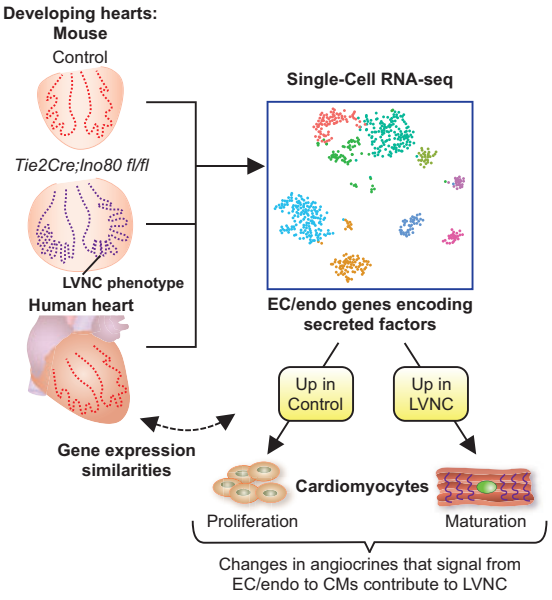

Single cell analysis of a mouse model of ventricular non-compaction and in vitro assays of cardiomyocyte growth demonstrated that coronary endothelial cells (ECs) normally promote myocardial compaction through secreted factors, but that endocardial and ECs can contribute to noncompaction under pathological conditions. EC, endothelial cells; endo, endocardial cells.

Keywords Single-cell RNA-sequencing • Left ventricular non-compaction • Angiocrine factors • Cardiomyocyte proliferation • Cardiomyocyte maturation

Introduction

Left ventricular non-compaction (LVNC) is a rare but potentially devastating disease, in which cardiac systolic function is compromised due to incomplete compaction of the ventricular wall.[1] Left ventricular non-compaction represents the third most prevalent form of congenital cardiomyopathy in the USA, manifesting in a myriad of cardiovascular complications such as heart failure, arrhythmias, and thromboembolism.[2] Like many congenital cardiomyopathies, the genetic basis of LVNC is highly complex and remains elusive. Genome-wide association studies have identified common gene mutations and molecular pathways related to sarcomere and sarcolemma function (e.g. MYH7, MYBPC3, TPM1, and TNNT2) in LVNC patients,[3,4] though such identified mutations are also found in dilated or hypertrophic cardiomyopathies and are not unique to LVNC.

Due to the limited understanding of the precise aetiology of the disease, there currently exists no therapeutic solutions that reverse the ventricular non-compaction phenotype.[2,5] Animal models of ventricular non-compaction to date have suggested that the pathology arises during embryonic development due to insufficient proliferation and premature maturation of cardiomyocytes from dysregulation of developmental signalling pathways such as transforming growth factor-beta (TGF-β) and Notch signalling.[1,6] Interestingly, a number of recent studies have found that the LVNC phenotype not only manifests in the myocardium but it is also highly correlated with improper endocardial function and/or development of the coronary endothelium.[7–10] For instance, endocardial/endothelial-specific deletion of *Fkbp1a* leads to myocardial non-compaction via up-regulation of endocardial Notch1 signalling, underlining the role of myocardium-to-endocardium paracrine signalling in controlling ventricular wall formation.[8] Additionally, dysregulation of Notch signalling in endocardial cells (ECs)[9,11] or presence of a single-nucleotide variant in MKL2 in vascular cells were shown to generate or contribute to LVNC, respectively.[10,12] These observations suggest the possibility that LVNC can arise from defects in cardiac endocardium and endothelium.

We previously reported that endothelial-specific deletion of the chromatin remodeller *Ino80* also results in an LVNC phenotype, where impaired coronary vessel angiogenesis coincided with non-compaction of the ventricular wall.[7] In contrast, myocardial development and compaction were unaffected when *Ino80* was deleted specifically in cardiomyocytes or in epicardial-derived stromal cells. In the *Tie2Cre;Ino80*$^{fl/fl}$ embryonic hearts exhibiting an LVNC phenotype, we observed that coronary vessel sprouting was compromised, which was coincident with increased E2F-mediated gene transcription and proliferation in endocardial and ECs.[7] We consequently hypothesize that when coronary angiogenesis cannot occur properly, it cannot provide paracrine or angiocrine factors that promote myocardial compaction whereas the remaining endocardium secretes factors that stimulate maturation and inhibit cardiomyocyte proliferation, leading to non-compaction of the myocardial wall.

Here, we use single-cell RNA-sequencing in *Tie2Cre;Ino80*$^{fl/fl}$ and wild-type counterpart embryonic hearts to identify candidate angiocrines expressed by endocardial and ECs during normal development and in LVNC conditions. We also assess the modulatory role of the identified secreted factors on cardiomyocyte proliferation and maturation in mouse heart development and in human-induced pluripotent stem cell (iPSC)-derived cardiomyocyte culture (*Graphical abstract*).

Methods

Mouse lines

The laboratory animal care programme at Stanford University is accredited by the Association for the Assessment and Accreditation of Laboratory Animal Care International (AAALAC Int'l). Experiments were conducted accordingly with NIH and Stanford University policies governing animal use and welfare. The mouse strains used in this study were: wild-type (CD1 and FVB, Charles River Laboratories), *Tie2Cre* (The Jackson Laboratories Stock number 004128), B6.CgTg(Tek-cre)12Flv/J, *Nfatc1Cre*, and *Ino80*^{flox}. For experiments, hemizygous Cre *Ino80*$^{flox/+}$ male mice were crossed with *Ino80*$^{fl/fl}$ females. Transgenic mice were on mixed backgrounds and ages (embryonic and adult) are indicated with each experiment. Both male and female embryos were included in analyses as we did not genotype for gender. When using the *AplnCreER* to excise the *Vegfr2* and *Ino80*, tamoxifen (4-OHT, H6278 Sigma) was dissolved in corn oil at a concentration of 20 mg/mL and injected into pregnant females by oral gavage at E12.5 and E13.5.

Embryonic heart explant culture

Whole ventricles were dissected from E12.5 mouse embryos. Samples were rinsed with cold Phosphate Buffered Saline (PBS) to remove blood cells and placed in 1:200 Matrigel (BD Biosciences) with EGM-2 MV media (Lonza, CC-4147, Basel, Switzerland) in 24-well plates (Costar, 3524) or cell culture inserts (MilliporeSigma, PI8P01250, Burlington, MA, USA). Explants were cultured in 5% O_2, 5% CO_2 at 37°C for 36 h before samples were fixed with 4% Paraformaldehyde (PFA) in PBS for 15 min. After fixation, explants were washed three times with 0.5% PBT (PBS + 0.5% Tween 20) and immunofluorescence staining was performed directly within the 24-well culture plates. Explants were incubated with primary antibodies in 0.5% PBT overnight at 4°C. Explants were washed with 0.5% PBT six times for 6 h and then incubated with corresponding secondary antibodies in 0.5% PBT overnight at 4°C. The day after, explants were washed three times and nuclei were counter-stained with 4′,6-diamidino-2-phenylindole (DAPI). After three washes in PBS, explants were imaged using an inverted Zeiss LSM-700 confocal microscope. Captured images were digitally processed using ImageJ (NIH) and Photoshop (Adobe Systems, Mountain View, CA, USA). Small-molecule inhibition was performed by the addition of 20 μM axitinib (Selleckchem, s1005, Houston, TX, USA) dissolved in Dimethyl sulfoxide (DMSO) directly to culture media after 1-day culture. An equal concentration of DMSO was added to the control media.

Human-induced pluripotent stem cell-derived cardiomyocyte culture

Human iPSCs from an LVNC patient and a healthy member were obtained from the Stanford Cardiovascular Institute iPSC Biobank. Induced pluripotent stem cells were cultured in E8 media (Gibco) for maintenance of pluripotency state. At 95% confluency, iPSCs were subjected to chemically defined cardiomyocyte differentiation protocol as previously described.[6] In brief, iPSCs were treated with 6 μM CHIR99021 (Selleckchem) in RPMI+B27 without insulin (Gibco) from Day 0 to 2. Media was changed to RPMI+B27 without insulin from Day 2 to 3, then the cells were treated with 5 μM IWR (Selleckchem) in RPMI+B27 without insulin from Day 3 to 5. Media was then changed to RPMI+B27 without insulin from Day 5 to 7. Robust beating of cardiomyocytes was observed starting at Day 8 of differentiation. From Day 7 and forward, iPSC-CMs were cultured in RPMI+B27 with insulin. Glucose starvation from Day 11 to 13 was used to eliminate non-cardiomyocyte cells. At Day 15, iPSC-CMs were transferred to Matrigel-coated chamber slides or 24-well plates at a sparse cell density and cultured at 5% O_2, 5% CO_2 at 37°C for 2 days. Preparation for immunostaining was performed as described above.

Statistical analysis

Statistical analyses were performed using Prism (GraphPad). Data are represented as mean ± SD. For animal knockout studies, no statistical methods were used to predetermine sample size; sample size was determined based on mouse genetics. Crosses were performed until a minimum of 3–10 experimental animals (i.e. mutants) from multiple litters were obtained. No randomization or blinding was performed for mouse crosses, but all quantifications were counted by a researcher blinded to genotype or treatment. Litter mate controls were always used for analysing experimental animals. Unpaired *t*-test (two-tailed) was performed to assess statistical significance between two sample groups. A $P < 0.05$ was considered statistically significant. Data from all experiments were included in the analyses presented. No experiments were omitted based on experimental outcomes, except for technical failures. Technical failures were rare, but always involved defective immunostaining, i.e. a complete absence of signal, and was due to expiring reagents. Power calculations for each experiment were performed to ensure that the numbers used have the power of 80% or greater to detect significant effect sizes ($\alpha = 0.05$). When experiments did not reach this threshold, experiments were repeated to include the appropriate *n*.

Results

Altered endocardial and cardiomyocyte transcriptomes in Ino80 mutant hearts with left ventricular non-compaction

To begin understanding how defective endothelial/endocardial cells may be involved in non-compaction of neighbouring myocardium, we performed scRNA-seq on dissected ventricles from *Tie2Cre;Ino80*$^{fl/+}$ and *Tie2Cre;Ino80*$^{fl/fl}$ hearts, the latter of which exhibits ventricular non-compaction phenotype (*Figure 1A*). We collected individual ventricular cells from embryonic day E15.5 hearts and performed droplet-based scRNA-seq using 10× Genomics Chromium platform. 518 *Tie2Cre;Ino80*$^{fl/+}$ and 576 *Tie2Cre;Ino80*$^{fl/fl}$ heart cells were used for downstream analysis (Supplementary material online, *Figure S1*). Unsupervised graph-based clustering identified nine expected cell populations (*Figure 1B*, Supplementary material online, *Figure S2*), which were annotated based on expression of known markers and included endocardial cells (*Npr3*+), coronary vessel ECs (*Cldn5*+, *Fabp4*+), smooth muscle cells/pericytes (*Pdgfrb*+), epicardium (*Apela*+), three fibroblast clusters (*Tcf21*+, *Col1a1*+, *Vcan*+), and two ventricular cardiomyocyte clusters (*Tnni1*+, *Ttn*+). All aforementioned cell types were observed in ventricular tissue of both genotypes (*Figure 1C*).

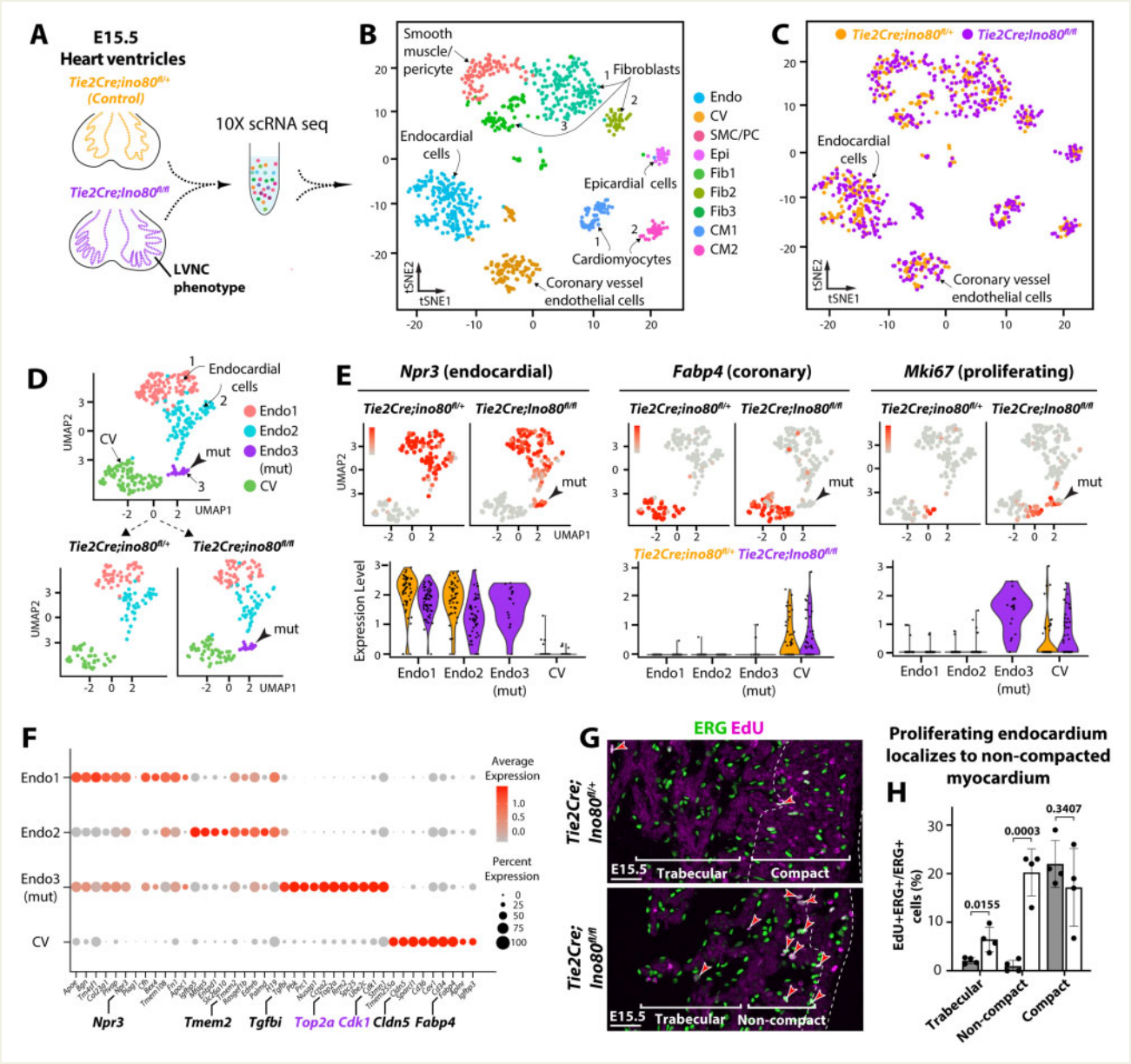

Figure 1 Single-cell mRNA-sequencing reveals mutant-specific cell states in *Tie2Cre;Ino80*$^{fl/fl}$ heart with left ventricular non-compaction. (*A*) Schematic of experiment, and (*B*) t-SNE visualization of cell populations identified in the two datasets combined. (*C*) tSNE visualization of *Tie2Cre;Ino80*$^{fl/+}$, and *Tie2Cre;Ino80*$^{fl/fl}$ cells. (*D*) UMAP analysis of endothelial and endocardial populations reveals a mutant-specific endocardial cell cluster (arrow, mut). (*E*) Feature and violin plots visualizing genes specific for endocardial, coronary vessel endothelial, and proliferating cells. Mutant-specific cluster represents proliferative endocardium. (*F*) Expression of top 10 genes that define each cluster. (*G*) EdU-positive endocardial cells (red arrows) are increased in mutant hearts and mostly localized to non-compacted myocardium. *Tie2Cre;Ino80*$^{fl/+}$, $n = 4$; *Tie2Cre;Ino80*$^{fl/fl}$, $n = 4$. (*H*) Quantification of G where each black dot represents the average of >3 FOVs from one heart. CM, cardiomyocytes; CV, coronary vessel ECs; Endo, endocardial cells; Epi, epicardial cells; Fib, fibroblasts; PC, pericytes; SMC, smooth muscle cells. Scale bars: 25 μm (*G*).

We next sub-clustered the endocardial and coronary endothelial populations to specifically investigate the differences between control and *Ino80* mutant vascular cells. Sub-clustering identified four clusters within this population—three were comprised of endocardial cells and one contained coronary endothelium (*Figure 1D*). One of the three endocardial clusters (Endo 3) contained only *Ino80*-deficient cells and no control cells (*Figure 1D*, lower panel). This mutant-specific cluster was defined in large part by high expression of proliferation genes, such as *Top2a* and *Cdk1*, which are very low in normal endocardium at this stage of development (*Figure 1E and F*, Supplementary material online, *Table S1*). Consistent with previous analyses from E12.5,[7] *in vivo* EdU-labelling and tissue sectioning revealed that these ectopically cycling endocardial cells primarily localized to non-compacted

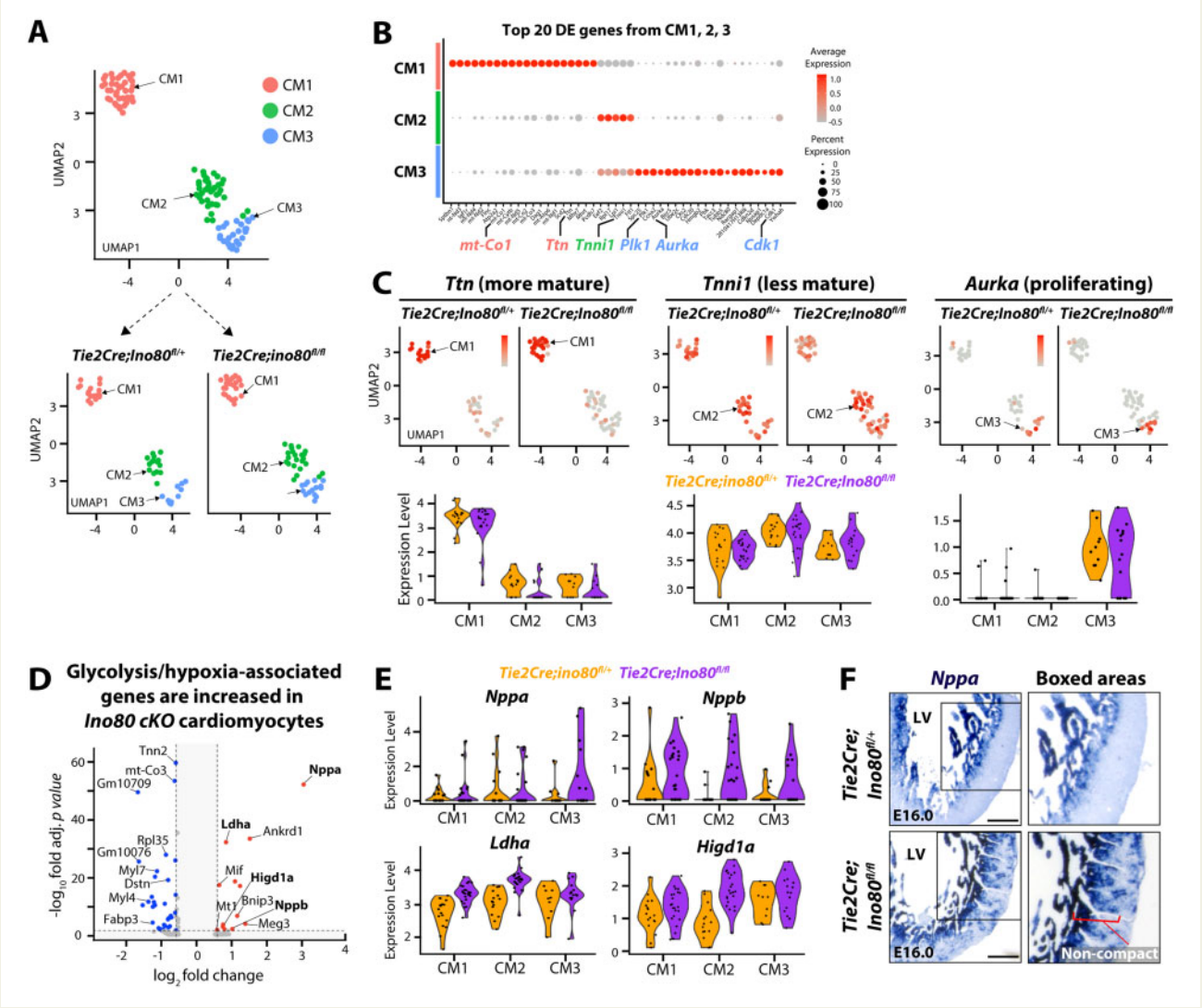

Figure 2 Effects of endothelial/endocardial deletion of *Ino80* on cardiomyocyte gene expression. (*A*) Sub-clustering of cardiomyocytes visualized on UMAPs. (*B*) Expression of top genes that define each sub-cluster. Highlighted genes suggest: CM1 = more mature, CM2 = less mature, CM3 = proliferating. (*C*) Feature and violin plots of select cardiomyocyte cluster-defining genes. (*D*) Volcano plot showing differentially expressed genes. Blue indicates decreased in mutant; red indicates increased in mutant where significance was considered <0.05 adjusted *P*-value evaluated by Poisson method. #Hypoxia-associated genes; *glycolysis-associated genes. (*E*) Violin plots of select genes showing how differences are spread over three cardiomyocyte clusters. (*F*) *In situ* hybridization validated *Nppa* expression changes. Images are representative of: *Tie2Cre;Ino80*$^{fl/+}$, $n = 3$; *Tie2Cre; Ino80*$^{fl/fl}$, $n = 3$ hearts. Scale bars: 25 μm.

myocardium at E15.5 (*Figure 1G and H*). Thus, this mouse model of ventricular non-compaction is coincident with the emergence of mutant-specific proliferative endocardial cells embedded within non-compacted myocardium.

Since the phenotype following endothelial/endocardial *Ino80* deletion is manifested in the myocardium, we next sub-clustered cardiomyocytes to observe transcriptional changes associated with non-compaction. Following sub-clustering, we observed three prominent cardiomyocyte subtypes, all of which contained cells from control and mutant hearts (*Figure 2A*). We first expected that the different clusters would represent compact and trabecular myocardium. However, known compact and trabecular marker genes did not distinguish the clusters. Instead, gene expression patterns indicated they were separated by maturity level and cell cycle. Specifically, cardiomyocyte cluster 1 (CM1) was defined by mature myocardial markers such as *Ttn*,[13] *Myh7*,[14] and *mt-Co1*,[15] and CM2 was defined by higher expression of markers found in immature myocardium in other studies such as *Tnni1*[16] (*Figure 2B and C*). CM3 was composed of cycling cells that also had lower expression of many of the CM2 genes (*Figure 2B and C*).

Genes that were differentially expressed between CMs from control and *Ino80*-deficient hearts were calculated (all CMs from each genotype were combined to increase statistical power). Thirty-nine genes were down-regulated in *Ino80*-deficient hearts and 13 were

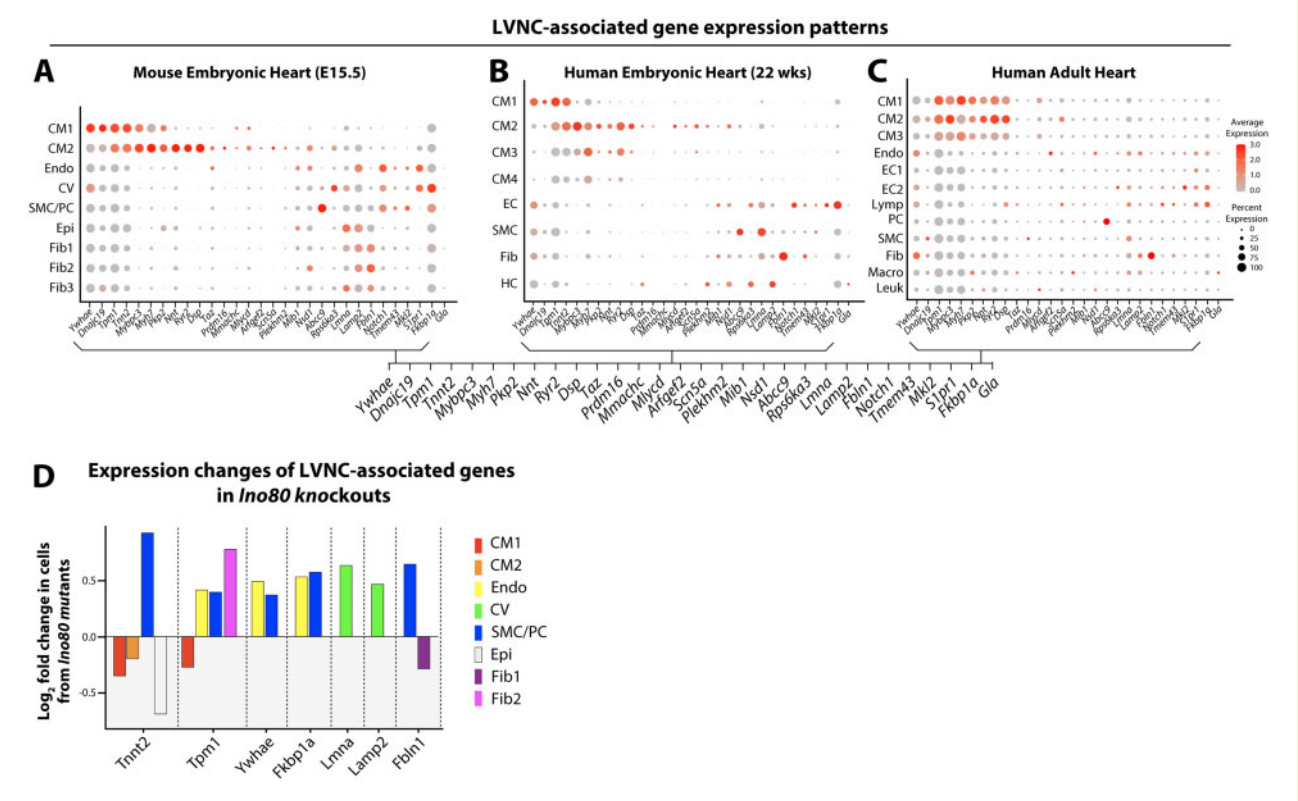

Figure 3 Left ventricular non-compaction-associated genes are expressed in multiple cell types in mouse and human hearts. (*A*) Dot plots showing expression of genes with reported genetic variants associated with human left ventricular non-compaction in the mouse heart, and (*B, C*) in the human embryonic (22-week post-gestation) and adult heart. (*D*) Left ventricular non-compaction-associated genes that change in *Ino80*-deficient hearts. CM, cardiomyocytes; CV, coronary vessel ECs; Endo, endocardial cells; Epi, epicardial cells; Fib, fibroblasts; HC, haematopoietic cells; Leuk, leukocytes; Macro, macrophages; PC, pericytes; SMC, smooth muscle cells.

up-regulated (*Figure 2D*). Gene set enrichment analysis to probe hallmark gene sets identified glycolysis, hypoxia, and fatty acid metabolism as being increased in mutants and gene classified as involved in development of skeletal muscle (myogenesis) to be down (Supplementary material online, *Table S2*). Specific genes in this pathway are highlighted in *Figure 2D and E*. Of the differentially expressed genes, *Nppa* was validated using *in situ* hybridization (*Figure 2F*). Although one limitation of these data is the low number of cells, we concluded that gene expression analysis indicates that cardiomyocyte metabolic state and development is dysregulated.

Left ventricular non-compaction-associated genes are expressed in multiple cardiac cell types

Our observations of *Tie2Cre;Ino80*$^{fl/fl}$ embryonic hearts indicate that primary defects in vascular cells can cause ventricular non-compaction in mice. To ascertain whether this is also possible in humans, we assessed in E15.5 mouse ventricles the expression of genes whose variants have been found in LVNC patients. We found that approximately one-third of the human LVNC-associated genes were expressed in embryonic mouse cardiomyocytes (*Figure 3A*). Interestingly, about half were specific to the more immature cluster, CM1, while the others were more prominently expressed in the more mature cluster, CM2. Another third was not highly expressed in cardiomyocytes, but instead found in various stromal cell types, including endocardial cells, coronary vessel ECs, mural cells, and fibroblasts (*Figure 3A*).

To investigate the relevance of these findings to human development, we analysed single-cell RNA-sequencing of a 22-week-old human foetal heart tissue. Expression patterns of LVNC genes in foetal human cardiac cells were similar to those observed in mice (*Figure 3A and B*). Furthermore, analysis of an independently generated adult human heart scRNA-seq dataset[17] revealed that the same set of LVNC-associated genes to be expressed in both cardiomyocytes and stromal cells (*Figure 3C*). A number of LVNC-associated genes expressed in foetal hearts, particularly those specific to cardiomyocytes, maintained their expression in the adult heart (*Figure 3C*). Finally, we investigated whether the genes associated with LVNC have significant expression level differences in *Ino80* mutant mice. Among these, seven genes were differentially expressed in at least one cell type in our model of LVNC (*Figure 3D*). These data indicate the possibility that LVNC-associated genes are derived from cells other than cardiomyocytes in humans and that they may be important for cardiac homeostasis and function in the adult.

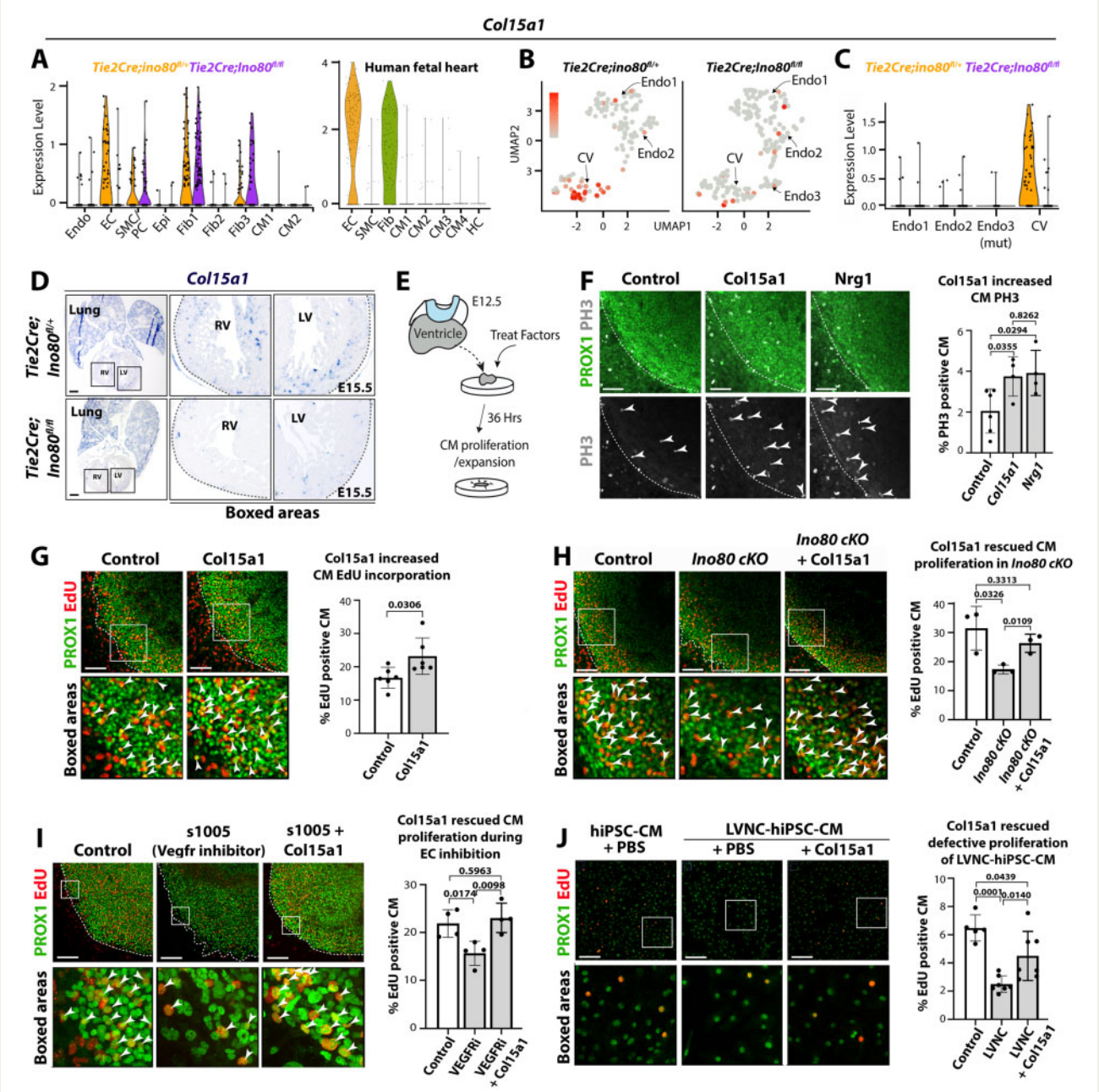

Figure 4 Col15a1 is decreased with left ventricular non-compaction and supports cardiomyocyte proliferation. (*A*–*C*) Violin and feature plots showing *Col15a1* expression. (*D*) *In situ* hybridization validates *Col15a1* decreased expression. *Tie2Cre;Ino80*$^{fl/+}$, $n = 4$ hearts; *Tie2Cre;Ino80*$^{fl/fl}$, $n = 4$ hearts. (*E*) Schematic outlining ventricle explant culture. (*F*–*I*) Confocal images and quantification of Col15a1-treated ventricle explants assayed for PH3 (*F*) and EdU incorporation (*G*–*I*). Col15a1 increased proliferation in PROX1+ cardiomyocytes (arrowheads) (*F*, *G*), which rescued the proliferative defects with *Ino80* knockout (*H*), and with EC depletion (*I*). (*J*) Col15a1 reversed defective proliferation in left ventricular non-compaction patient-specific induced pluripotent stem cell-cardiomyocytes In bar graphs in (*F*–*J*), each black dot represents the average value from >3 FOVs from individual hearts. CM, cardiomyocytes; CV, coronary vessel ECs; Endo, endocardial cells; Epi, epicardial cells; Fib, fibroblast; HC, haematopoietic cells; PC, pericytes; SMC, smooth muscle cells; VEGFRi, VEGFR inhibitor. Scale bars: 50 μm (*B*); 100 μm (*C*–*J*).

Col15a1 is expressed in coronary ECs and stimulates cardiomyocyte proliferation

Our previous study showed that ECs stimulate cardiomyocyte proliferation, a behaviour critical for ventricular compaction, independent of blood flow, and in an *Ino80*-dependent manner.[7] We hypothesized that this activity was mediated through a factor specifically secreted by coronary ECs that was decreased in *Ino80* mutants.[7] We therefore analysed our scRNA-seq data to first identify genes for secreted proteins (defined by Uniprot) that were expressed in coronary ECs and not in the endocardium, which resulted in 15 potential candidates. In particular, we found *Col15a1* to be significantly down-regulated in *Ino80*-deficient coronary ECs (Supplementary material online, *Table S3*). *Col15a1* was normally expressed in coronary ECs, smooth muscle cells, and fibroblasts in mouse hearts and in coronary ECs and fibroblasts in human hearts (*Figure 4A*), but it was only significantly decreased in *Ino80*-deficient coronary ECs (*Figure 4A–C*) as validated by *in situ* hybridization on E15.5 hearts (*Figure 4D*). These data indicate that endothelial deletion of *Ino80* impairs expression of *Col15a1* in coronary vessels, which may play a role in ventricular non-compaction.

We next assessed the effect of recombinant Col15a1 on cardiomyocyte proliferation by culturing explanted mouse embryonic heart tissue. Explanted E12.5 mouse heart ventricles were cultured on a dish for 1 day, then treated with recombinant proteins or a vehicle control for 36 h prior to fixation and immunostaining[7] (*Figure 4E*). Proliferation was assessed by either phospho-H3 or EdU immuno staining, and cardiomyocyte nuclei were identified by nuclear localization of Prox1[7,18] (Supplementary material online, *Figure S3*). Exogenous treatment of Col15a1 increased proliferation of wild-type mouse cardiomyocytes within explant cultures observed from phospho-H3 localization (*Figure 4F*) and EdU incorporation (*Figure 4G*), which reached proliferative levels similar to that induced by Nrg1[19] (*Figure 4F*). Col15a1 also partially rescued the reduced proliferative rate we previously found to be characteristic of ventricles from *Tie2Cre;Ino80*$^{fl/fl}$ mice (*Figure 4H*) and heart explants exposed to the vascular endothelial growth factor receptor (VEGFR) inhibitor s1005, which inhibits coronary EC growth[7] (*Figure 4I*).

Previously, we have shown that iPSC-derived cardiomyocytes (iPSC-CMs) from LVNC patients exhibit reduced proliferative capacity.[6,20] To determine whether Col15a1 also stimulates cardiomyocyte proliferation in human cardiomyocytes, we treated LVNC iPSC-CMs with exogenous Col15a1 and observed Col15a1 increased proliferation of LVNC iPSC-CMs to levels more similar to that of iPSC-CMs from a healthy family member (*Figure 4J*). Taken together, our data suggest coronary vessel-derived Col15a1 promotes myocardial proliferation, and that its decrease in *Ino80*-deficient embryonic hearts could contribute to the non-compaction phenotype.

Defective endocardium expresses secreted factors that inhibit cardiomyocyte proliferation and stimulate maturation

As we found a mutant-specific endocardial cell cluster within the non-compacted myocardium, we hypothesized that these cells may secrete factors that affect neighbouring cardiomyocytes during compaction. We identified *Tgfbi, Igfbp3, Isg15*, and *Adm* (*Figure 5A*, Supplementary material online, *Figure S4* and *Table S3*) to be significantly up-regulated in *Ino80* mutant endocardial and ECs, which encode secreted proteins. The increase in expression of these genes was not specific to the Endo 3 cluster, but also occurred in other endocardial clusters and coronary endothelium (*Figure 5A*), and, in the case of *Igfbp3*, the epicardium (Supplementary material online, *Figure S4*). We were particularly intrigued by the gene *Tgfbi*, or TGF-β induced, as we have previously shown that human LVNC iPSC-CMs exhibit dysregulated TGF-β signalling.[6]

We next validated the up-regulation of the four genes using *in situ* hybridization. *Tgfbi* localization in *Tie2Cre;Ino80*$^{fl/+}$ and *Tie2Cre;Ino80*$^{fl/fl}$ hearts at E15.5 revealed that, while its expression was similar in the lung, mutant endocardial cells within non-compacted myocardium (i.e. *Nppa*+) had increased mRNA levels (*Figure 5B*). *Tie2Cre;Ino80*$^{fl/+}$ and *Tie2Cre;Ino80*$^{fl/fl}$ hearts both express *Tgfbi* at E12.5 when the ventricular wall is mostly trabeculae, with qualitatively greater expression in mutants (*Figure 5C*). As the majority of the endocardial cells in the *Tie2Cre;Ino80*$^{fl/+}$ hearts down-regulated *Tgfbi* by E13.5, the mutant endocardial cells maintained the high expression of *Tgfbi* (*Figure 5C*). A time course of another gene increased in mutant endocardium, *Igfbp3*, showed the different pattern that there is little endocardial expression in either genotype at E12.5, but its expression increased in mutants at later time points (*Figure 5D*). We also confirmed that the expression of *Isg15* and *Adm* was increased in mutant ventricles (Supplementary material online, *Figure S5*). Thus, these genes constitute a list of secreted factors whose expression is positively correlated with ventricular non-compaction in mice.

We next aimed to address whether these gene expression changes were a direct consequence of *Ino80* deletion or perhaps a tissue level response to impaired coronary angiogenesis and/or ventricular non-compaction (e.g. hypoxia). We cross-referenced the scRNA-seq gene list with bulk RNA-seq data from cultured cells and earlier staged *Tie2Cre;Ino80*$^{fl/fl}$ hearts (E13.5 and E14.5) that are not yet as severely impacted.[7] This included bulk RNA-seq performed on cultured human umbilical vein ECs (HUVECs) that were transfected with either control or *Ino80*-specific siRNA and whole E13.5 and E14.5 mutant hearts.[7] *Tgfbi* and *Isg15* were increased in both *Ino80* knockdown human umbilical vein ECs and mutant hearts. However, *Igfbp3* and *Adm* were not changed or decreased in both experiments (*Figure 6A*). These observations support the idea that *Isg15* and *Tgfbi* might be directly regulated by *Ino80* while *Igfbp3* and *Adm* up-regulation could be a consequence of hypoxia, which is consistent with their known function of being hypoxia-inducible genes.[21–23]

We next tested the hypothesis that the secreted factors up-regulated in *Ino80*-deficient endocardial and coronary ECs inhibit compaction using both mouse and human cardiomyocytes. As above, we utilized *ex vivo* assays of cardiomyocyte behaviour. In addition to decreased cardiomyocyte proliferation,[7] non-compaction is associated with decreased cardiomyocyte packing (Supplementary material online, *Figure S6*) and premature sarcomere maturation as indicated by increased striation development.[7,24,25] For the mouse *ex vivo* and human *in vitro* cardiomyocyte experiments, two general treatments were given, either one of the identified factors individually (*Tgfbi, Igfbp3, Isg15*, or *Adm*) or a cocktail of all factors together (4 factors or '4F').

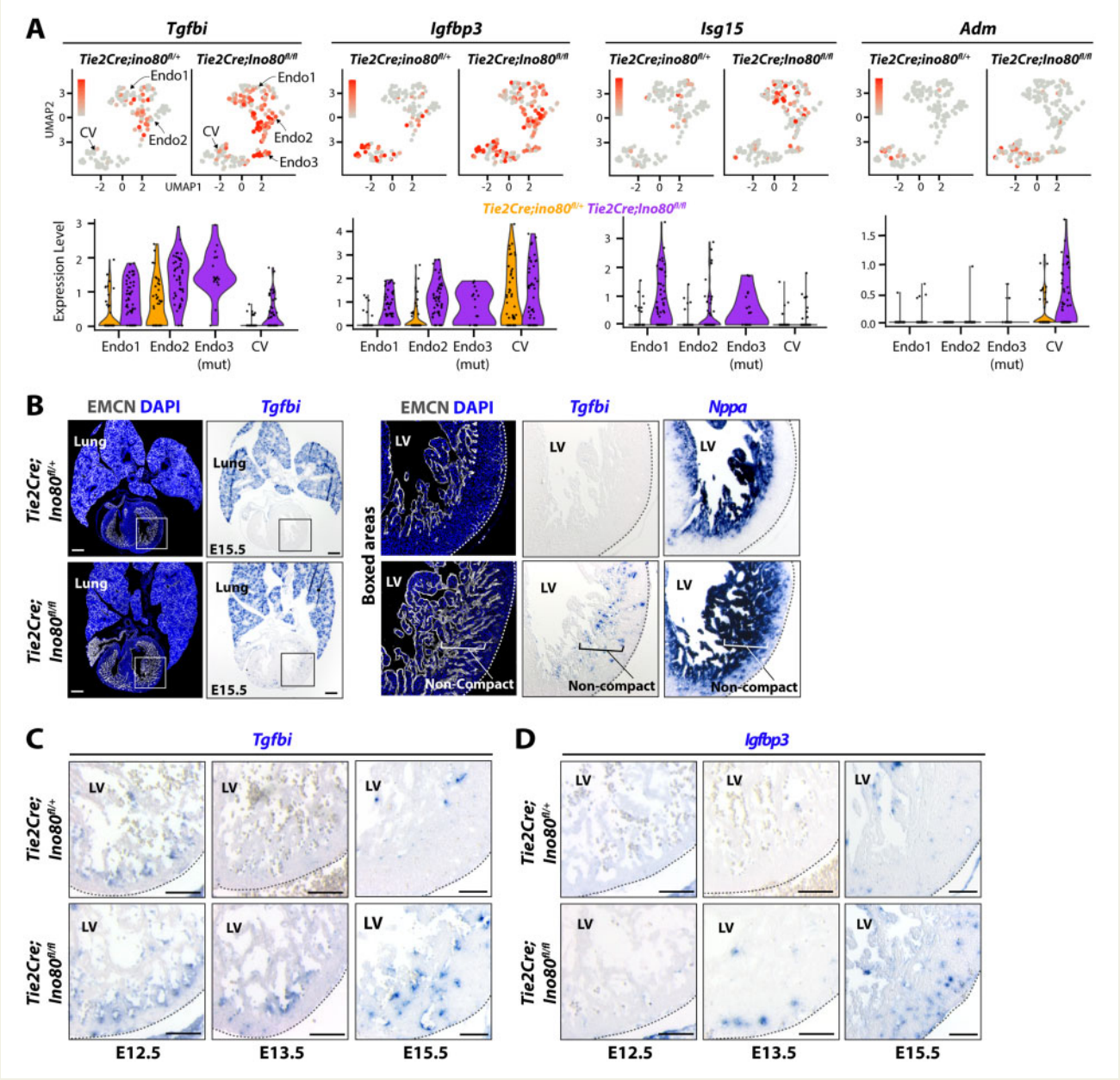

Figure 5 *Ino80*-deficient endocardial and ECs increase expression of secreted proteins. (*A*) Feature and violin plots of secreted factors whose expression was increased in *Ino80* mutants. (*B*) *In situ* hybridization validated *Tgfbi* expression. Expanded EMCN+ endocardium and *Nppa* expression mark non-compacted myocardium. *Tie2Cre;Ino80*$^{fl/+}$, $n = 4$; *Tie2Cre;Ino80*$^{fl/fl}$, $n = 4$. (*C*, *D*) *In situ* hybridization on left ventricles (LV) for *Tgfbi* and *Igfbp3* at indicated developmental stages. *Tie2Cre;Ino80*$^{fl/+}$, $n = 4$ hearts; mutant, $n = 4$ hearts. Scale bar: 100 μm (*B*); 25 μm (*C*, *D*).

To investigate the exogenous effects of the four factors on cardiomyocyte proliferation, *ex vivo* mouse embryonic heart tissue cultures were prepared and analysed as described above (*Figure 4E*). Phospho-H3 immunostaining showed that Tgfbi and Isg15 decreased cardiomyocyte proliferation (*Figure 6B*). EdU assays showed that cardiomyocyte proliferation was significantly decreased with application of 4F or each factor individually (*Figure 6C*). When the iPSC-CMs were treated with 4F secreted factor cocktail or individually with each one of the four factors on Day 15 of differentiation, we similarly observed a decrease in the proliferation of the cells (*Figure 6D*).

Structural changes associated with non-compaction were also investigated. It was noted that cardiomyocytes from explants treated with 4F or individual factors were less densely packed than controls (*Figure 6E*). The average distance between nuclei has been previously used to measure cell packing,[26,27] and this analysis revealed an increase in nuclear distance and decrease in cell packing in non-compacted myocardium *in vivo* (Supplementary material online, *Figure S6*). Using this metric to quantify explant cultures, we observed the same phenomenon upon application of either 4F or individual factors—they increased nuclei distance and a

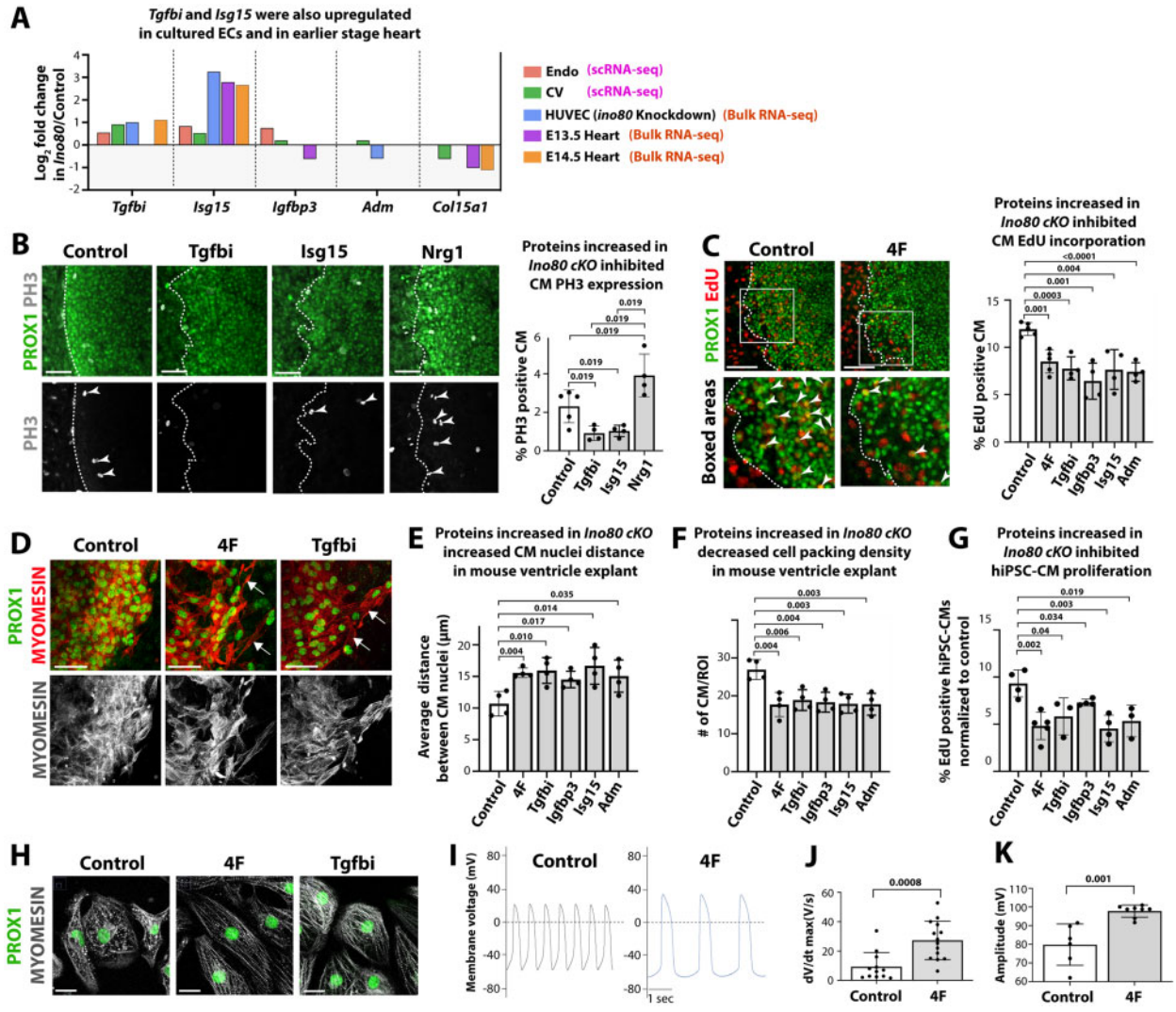

Figure 6 Secreted proteins up-regulated in *Ino80* mutants inhibit cardiomyocyte proliferation and stimulate maturation. (*A*) Comparing scRNA-seq with bulk RNA-seq datasets from human umbilical vein ECs treated with *Ino80* siRNA and whole hearts from earlier time points (E13.5 and E14.5). *Tgfbi* and *Isg15* are up-regulated in cells and earlier hearts suggesting the change is not secondary to tissue hypoxia while *Igfbp3* and *Adm*, known hypoxia-inducible genes, are not. (*B, C*) Confocal images and quantification of heart ventricle explants assessed for PH3 (*B*) or EdU incorporation (*C*). PROX1+ proliferating cardiomyocytes (arrowheads) are decreased by factors. (*D*) EdU-labelling showed that treatment of 4F cocktail decreased proliferation in control induced pluripotent stem cell-cardiomyocytes (*E*) Myomesin and PROX1 immunofluorescence revealed spreading of cardiomyocytes (arrows) in mouse ventricle explant cultures with indicated treatments. (*F*) Quantification of distance between cardiomyocytes, and (*G*) packing density of cells. (*H*) Left ventricular non-compaction induced pluripotent stem cell-cardiomyocytes treated with 4F or Tgfbi exhibited elongated morphology with more organized sarcomeric structure. (*I*) Electrophysiological measurements of spontaneous action potentials by patch clamping of single-induced pluripotent stem cell-cardiomyocytes shows 4F treatment increased maximum upstroke velocity (*J*) and action potential amplitude (*K*). Bar graphs show *N* for each experiment as a black dot. CV, coronary vessel ECs; Endo, endocardial cells; HUVEC, human umbilical vein EC. Scale bars: 50 μm (*B*); 75 μm (*C*); 100 μm (*E, H*).

decreased cell packing (*Figure 6E–G*). Therefore, these secreted factors induce a 'spreading' of myocardium similar to that seen in non-compacted hearts.

Another structural change we found to be characteristic of non-compacted myocardium was premature cardiomyocyte maturation. Specifically, cardiomyocytes from *Ino80* mutant hearts exhibited more organized sarcomeres than controls at inappropriately early developmental stages.[7] Immunofluorescence for the sarcomeric protein myomesin on 4F-treated and control iPSC-CMs showed that both 4F and Tgfbi transformed the cells from circular with punctate myomesin to elongated with more aligned sarcomeres, which is a hallmark of maturation (*Figure 6H*). Thus, secreted factors whose expression was increased in Ino80-deficient endocardial and ECs suppress cardiomyocyte proliferation, a hallmark feature of ventricular non-compaction. Another feature of cardiomyocyte maturation is a change in electrophysiological properties. Action potential (AP)

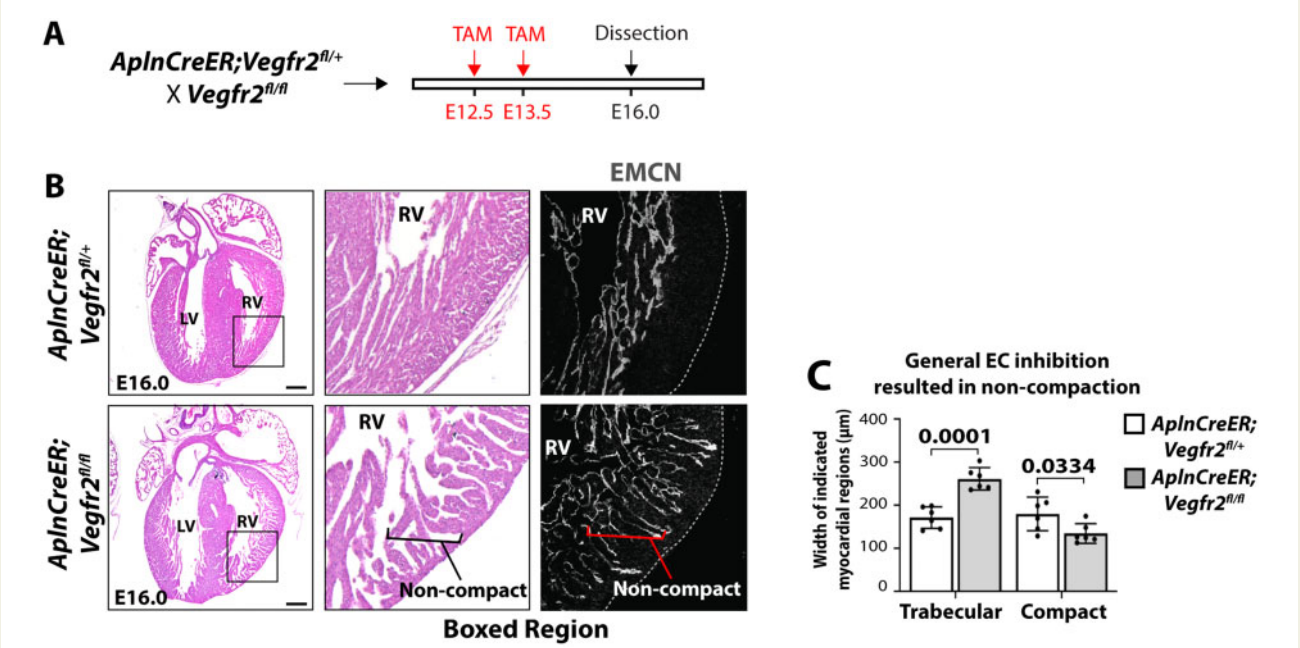

Figure 7 Inhibited coronary vessel growth leads to myocardial non-compaction. (*A*) Schematic showing experimental strategy to specifically inhibit coronary vessel growth. (*B*) Haematoxylin and eosin staining reveals non-compaction in *AplnCreER;Vegfr2*$^{fl/fl}$ hearts. *AplnCreER;Ino80*$^{fl/+}$, $n = 6$ hearts; *AplnCreER;Ino80*$^{fl/fl}$, $n = 6$ hearts at E16.0. (*C*) Quantification of compact and trabecular myocardium. Each black dot in bar graphs represents the average value from >3 FOVs from one heart. Scale bars: 100 μm (*B*).

recordings performed by patch-clamp showed that 4F treatment increased the maximum upstroke velocity and the AP amplitude compared with the non-treated cells (*Figure 6I–K*). Moreover, the resting membrane potential of treated cells shifted from -60 to -70 mV, a consequence of increased current through IK1 channels.[28] These changes to AP and resting membrane potential indicate an enhancement of electrophysiological maturity. Taken together, these data show that, in culture, endocardial-derived factors overexpressed in *Ino80*-mutant ECs can drive the structural phenotypes seen in non-compacted hearts.

General inhibition of coronary angiogenesis recapitulates non-compaction

Our observation that coronary vessels express a gene for a secreted factor that stimulates cardiomyocyte proliferation suggests that general coronary angiogenesis could lead to non-compaction, irrespective of Ino80. To test this possibility, we specifically inhibited coronary angiogenesis using a different genetic model and analysed ventricular wall development. *AplnCreER* was used to delete VEGFR2 at E12.5 and E13.5 and analysis performed at E16.5 (*Figure 7A*). *AplnCreER* is specific to coronary ECs in the developing heart[29] and VEGFR2 is required for general EC growth, allowing us to specifically inhibit coronary angiogenesis without affecting the endocardium. Quantification of trabecular and compact myocardial width in these animals at E16.5 revealed a defect in compact expansion at the expense of over-developed trabeculae (*Figure 7B and C*). This is a hallmark of the non-compaction phenotype, and, therefore, we concluded general coronary vessel inhibition can lead to non-compaction in mice.

Adult phenotype of embryos exhibiting non-compaction

We next sought to understand whether the dramatic embryonic phenotype we detected with *Tie2Cre;Ino80*$^{fl/fl}$ resulted in cardiac disease in the adult. To this end, we allowed animals grow to adulthood and observed heart wall morphology and cardiac function. We first noted a profound lethality with *Tie2Cre;Ino80*$^{fl/fl}$ animals so that there were not enough adult animals of this genotype to perform a meaningful analysis (*Figure 8A*). This lethality could result from the severe ventricular non-compaction observed in these animals, but since this is a constitutive pan-endothelial Cre that also recombines in the haematopoietic system, we cannot exclude impacts on other vascular beds and blood cells. We instead decided to use a more specific Cre, *Nfatc1Cre*, which is specific to endocardial cells in the heart.[30,31] Endocardial cells give rise to a large subset of coronary vessels, and *Nfatc1Cre;Ino80*$^{fl/fl}$ mice exhibit evidence of non-compaction, although with much less severity.[7] *Nfatc1Cre;Ino80*$^{fl/fl}$ mice survived at expected frequencies (*Figure 8A*), and we therefore performed histological analysis and cardiac phenotyping on adults. Basic histological analyses using H&E staining revealed that *Nfatc1Cre;Ino80*$^{fl/fl}$ hearts did not have extensive trabeculations, but almost all were larger in size than *Nfatc1Cre;Ino80*$^{fl/+}$ hearts (*Figure 8B*). Echocardiography revealed that cardiac systolic function was significantly impaired. Left ventricular ejection fraction was decreased and end-diastolic volume and left ventricular mass were increased (*Figure 8C and D*), which were consistent with histological findings (*Figure 8B*). These data

A

Cre line (no. mice)	Control Cre- Ino80fl/+ (25%)	Control Cre- Ino80fl/fl (25%)	Het Cre+ Ino80fl/+ (25%)	cKO Cre+ Ino80fl/fl (25%)
Tie2Cre (69)	27.54%	28.99%	40.58%	2.89%
Nfatc1Cre (35)	22.86%	22.86%	28.57%	25.71%

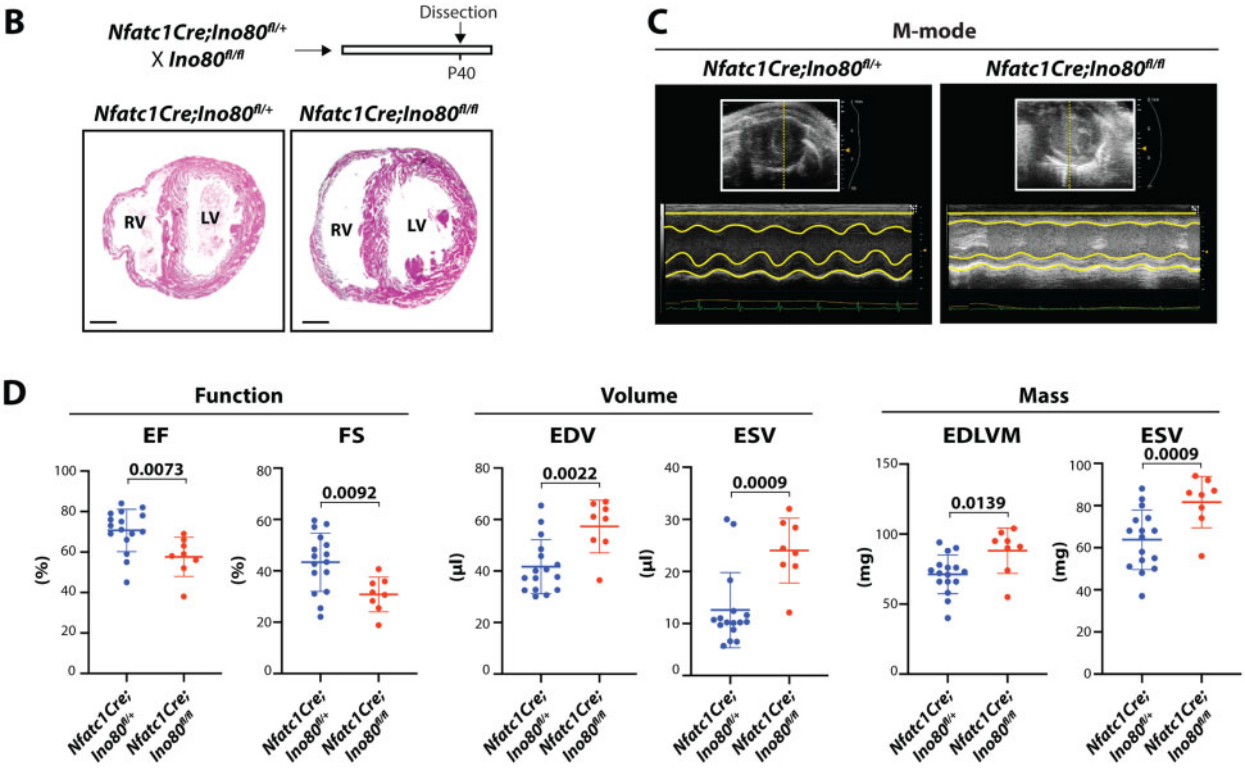

Figure 8 *Ino80* deletion in endocardium disrupts ventricular systolic function of adult mouse hearts. (*A*) Number of animals recovered at weaning for the indicated genotypes. (*B*) H&E staining revealed that *Nfatc1Cre;Ino80*$^{fl/fl}$ mice exhibit dilated heart morphology. *Nfatc1Cre;Ino80*$^{fl/+}$, $n = 3$ hearts; *Nfatc1Cre;Ino80*$^{fl/fl}$, $n = 3$ hearts at P40. (*C*) M mode images acquired at the mid-papillary segment of the left ventricle (LV) during echocardiography at postnatal Day 40. (*D*) Left ventricular function assessment. EDLVM, end-diastolic left ventricular mass; EDV, end-diastolic volume; EF, ejection fraction; ESLVM, end-systolic left ventricular mass; ESV, end-systolic volume; FS, fractional shortening. Scale bars: 100 µm (*B*).

show that endocardial and partial coronary EC deletion of *Ino80*, which causes a mild form of embryonic ventricular non-compaction,[7] leads to dysfunction in adult hearts.

Discussion

Here, we used a mouse model with endothelial genetic insufficiency (EC-specific *Ino80* deletion) to study the potential role of vascular-derived factors in normal and pathological heart wall growth. We performed scRNA-seq of *Ino80* mutant hearts to investigate the cell state changes that accompany LVNC and to precisely characterize cell-type-specific changes in gene expression. This analysis revealed a new endocardial cell state specific to *Ino80* mutant hearts that was characterized by an increase in proliferation genes, which localized to non-compacted myocardium. We also used the scRNA-seq data, as well as additional human datasets, to investigate which cells express genes associated with human LVNC. The results showed that LVNC-associated genes are expressed in both cardiomyocytes and the other stromal cell types within the heart. Thus, scRNA-seq analysis revealed that perturbations in endocardial and ECs accompany ventricular non-compaction in mice and suggested potential sites of origins for the human disease.[32]

Using scRNA-seq to identify gene expression differences within specific cell types, we identified five candidate secreted factors that endocardial or coronary ECs might use to influence cardiomyocyte behaviour. Among these was *Col15a1*, which was expressed by coronary vessel ECs and was decreased in *Ino80* mutants, suggesting it might function to support cardiomyocyte proliferation. In murine explant cultures, recombinant Col15a1 stimulated cardiomyocyte

proliferation. Application of Col15a1 to explant cultures that mimic LVNC—*Ino80* deficient or treated with VEGFR2 inhibitor—rescued proliferation defects. It also rescued the poor proliferative response of iPSC-CMs derived from a patient with LVNC. Little is known about the molecular function of Col15a1, but it is mostly found in the basement membrane of capillary ECs and smooth muscle cells.[33–35] Adult *Col15a1* constitutive knockout mice are viable, but exhibit progressive evidence of muscular disease, including cardiac function deficiencies and cardiomyocyte structural defects.[36,37] Col15a1 has also been shown to bind to fibronectin and laminin to influence cell adhesion,[38] and thus these two cell types may be working together to produce an extracellular matrix environment that promotes cardiomyocyte proliferation and, as a result, support compaction. Future experiments will delve into precisely how Col15a1 stimulates cardiomyocyte proliferation.

Comparing differential expression also identified several genes highly up-regulated in Ino80-deficient endocardial cells and coronary ECs. This caused us to consider the hypothesis of a disease-promoting function. This is a reasonable role for the endocardium since it was overrepresented in Ino80 mutants where it lined non-compacted myocardium. Indeed, even in normal hearts, endocardial cells are associated with non-proliferative trabecular myocardium. The proteins encoded by the up-regulated genes—Tgfbi, Igfbp3, Isg15, and Adm—reduced proliferation of mouse and human cardiomyocytes and induced phenotypic changes, such as elongated morphology with increased sarcomere formation and physiological maturation, consistent with it facilitating the onset of the LVNC phenotype.

These four factors carry out a variety of functions. TGFBI is a secreted protein that has been reported to bind to a variety of extracellular matrix molecules and interacts with integrins through its C-terminal RGD domain.[39–41] Integrins are highly expressed in cardiomyocytes,[42,43] and are known to be involved in sarcomere assembly and maturation.[44] IGFBP3 can bind and inhibit the function of insulin-like growth factors (IGFs),[45] which stimulate cardiomyocyte proliferation.[46] IGFBP3 has also been shown to bind the cell surface receptor LRP1[47] and be internalized and perform various intercellular functions.[48] Ubiquitin-like protein ISG15 is known to be strongly induced by type I interferons and can covalently conjugate itself to potentially hundreds of targets to regulate their function.[49–51] Finally, ADM is a peptide hormone that is secreted by endothelial and vascular smooth muscle cells and has been reported to have protective effects in many pathological conditions, including cardiac hypertrophy, myocardial infarction, and atherosclerosis.[52,53] It has been reported to directly bind cardiomyocytes through its receptors e.g. CRLR and RAMPs, although the downstream consequences of signalling have yet to be investigated.[54,55] It will thus be necessary to explore their precise role in regulating cardiomyocyte behaviour in compacting mouse hearts and in the human iPSC-CMs.

Consistent with the hypoxic hallmark in cardiomyocytes from *Ino80* mutant hearts, two of the genes up-regulated in *Ino80* mutant endocardium and/or endothelium (*Igfbp3* and *Adm*) are known to be hypoxia-inducible and their change was not seen in non-hypoxic *Ino80* knockdown cell culture experiments or in bulk RNA-seq from stages that should be prior to onset of hypoxia. Their hypoxia inducibility along with their effects on cardiomyocytes suggests the possibility that an initial hypoxic state might start a pathologic feedback loop that exacerbates non-compaction.

In summary, we identified a novel set of endothelial- and endocardial-expressed secreted during cardiac development that simultaneously modulates cardiomyocyte proliferation and maturation, two key cellular processes critical for ventricular compaction. These findings shed light into an unprecedented aetiology of LVNC, whereby dysregulation of paracrine signalling of non-cardiomyocyte cell types can lead to reduced cardiomyocyte proliferation and myocardial non-compaction. Consequently, further elucidation of these phenomena will be necessary to develop effective patient-specific therapeutics to combat the complex pathological nature of LVNC.

Supplementary material

Supplementary material is available at *European Heart Journal* online.

Acknowledgements

This work was supported by the imaging instruments and image analysis provided by the Stanford Center for Innovation in *In vivo* Imaging (SCi3) service centre at Stanford University.

Funding

This work was supported by the NIH (K99 HL150216 to D.T.P.; R01 HL113006, R01 HL130020, R01 HL141371, R01 HL145676, and P01 HL141084 to J.C.W.; R01-HL128503 to K.R.-H., R35 GM119580 to A.J.M, T32 HL098049 to D.N.), California Institute for Regenerative Medicine Bridges Master's Training Grant (CIRM EDUC2-08391 to J.Y.Y.), and the New York Stem Cell Foundation (NYSCF-Robertson Investigator to K.R.-H.). Additional seed funding from Stanford Cardiovascular Institute was provided to A.J.M. We are grateful for funding support from the University of Toronto Clinician Scientist Training Program and Detweiler Traveling Fellowship from the Royal College of Physicians and Surgeons (M.C.).

Conflict of interest: none declared.

Data availability

Bulk RNA sequencing data are publicly available at GEO:GSE152887. The accession number for single cell RNA sequencing data reported in this paper is GEO Databases: GSE175589 (https://www.ncbi.nlm.nih.gov/geo/query/acc.cgi?acc=GSE175589). The secure token ovgloyiyptofdud has been created to allow review of record GSE175589 while it remains in private status. We will release the data immediately once the final decision is made.

References

1. Finsterer J, Stollberger C, Towbin JA. Left ventricular noncompaction cardiomyopathy: cardiac, neuromuscular, and genetic factors. *Nat Rev Cardiol* 2017;**14**:224–237.
2. Lee TM, Hsu DT, Kantor P, Towbin JA, Ware SM, Colan SD, Chung WK, Jefferies JL, Rossano JW, Castleberry CD, Addonizio LJ, Lal AK, Lamour JM, Miller EM, Thrush PT, Czachor JD, Razoky H, Hill A, Lipshultz SE. Pediatric cardiomyopathies. *Circ Res* 2017;**121**:855–873.
3. Sedaghat-Hamedani F, Haas J, Zhu F, Geier C, Kayvanpour E, Liss M, Lai A, Frese K, Pribe-Wolferts R, Amr A, Li DT, Samani OS, Carstensen A, Bordalo DM, Müller M, Fischer C, Shao J, Wang J, Nie M, Yuan L, Haßfeld S, Schwartz C, Zhou M, Zhou Z, Shu Y, Wang M, Huang K, Zeng Q, Cheng L, Fehlmann T, Ehlermann P, Keller A, Dieterich C, Streckfuß-Bömeke K, Liao Y, Gotthardt M,

Katus HA, Meder B. Clinical genetics and outcome of left ventricular non-compaction cardiomyopathy. *Eur Heart J* 2017;**38**:3449–3460.
4. van Waning JI, Moesker J, Heijsman D, Boersma E, Majoor-Krakauer D. Systematic review of genotype-phenotype correlations in noncompaction cardiomyopathy. *J Am Heart Assoc* 2019;**8**:e012993.
5. van Waning JI, Caliskan K, Hoedemaekers YM, van Spaendonck-Zwarts KY, Baas AF, Boekholdt SM, van Melle JP, Teske AJ, Asselbergs FW, Backx A, Du Marchie Sarvaas GJ, Dalinghaus M, Breur J, Linschoten MPM, Verlooij LA, Kardys I, Dooijes D, Lekanne Deprez RH, As IJ, van den Berg MP, Hofstra RMW, van Slegtenhorst MA, Jongbloed JDH, Majoor-Krakauer D. Genetics, clinical features, and long-term outcome of noncompaction cardiomyopathy. *J Am Coll Cardiol* 2018;**71**:711–722.
6. Kodo K, Ong SG, Jahanbani F, Termglinchan V, Hirono K, InanlooRahatloo K, Ebert AD, Shukla P, Abilez OJ, Churko JM, Karakikes I, Jung G, Ichida F, Wu SM, Snyder MP, Bernstein D, Wu JC. iPSC-derived cardiomyocytes reveal abnormal TGF-beta signalling in left ventricular non-compaction cardiomyopathy. *Nat Cell Biol* 2016;**18**:1031–1042.
7. Rhee S, Chung JI, King DA, D'amato G, Paik DT, Duan A, Chang A, Nagelberg D, Sharma B, Jeong Y, Diehn M, Wu JC, Morrison AJ, Red-Horse K. Endothelial deletion of Ino80 disrupts coronary angiogenesis and causes congenital heart disease. *Nat Commun* 2018;**9**:368.
8. Chen H, Zhang W, Sun X, Yoshimoto M, Chen Z, Zhu W, Liu J, Shen Y, Yong W, Li D, Zhang J, Lin Y, Li B, VanDusen NJ, Snider P, Schwartz RJ, Conway SJ, Field LJ, Yoder MC, Firulli AB, Carlesso N, Towbin JA, Shou W. Fkbp1a controls ventricular myocardium trabeculation and compaction by regulating endocardial Notch1 activity. *Development* 2013;**140**:1946–1957.
9. D'Amato G, Luxán G, del Monte-Nieto G, Martínez-Poveda B, Torroja C, Walter W, Bochter MS, Benedito R, Cole S, Martinez F, Hadjantonakis A-K, Uemura A, Jiménez-Borreguero LJ, de la Pompa JL. Sequential Notch activation regulates ventricular chamber development. *Nat Cell Biol* 2016;**18**:7–20.
10. Gifford CA, Ranade SS, Samarakoon R, Salunga HT, de Soysa TY, Huang Y, Zhou P, Elfenbein A, Wyman SK, Bui YK, Cordes Metzler KR, Ursell P, Ivey KN, Srivastava D. Oligogenic inheritance of a human heart disease involving a genetic modifier. *Science* 2019;**364**:865–870.
11. Luxán G, Casanova JC, Martínez-Poveda B, Prados B, D'Amato G, MacGrogan D, Gonzalez-Rajal A, Dobarro D, Torroja C, Martinez F, Izquierdo-García JL, Fernández-Friera L, Sabater-Molina M, Kong Y-Y, Pizarro G, Ibañez B, Medrano C, García-Pavía P, Gimeno JR, Monserrat L, Jiménez-Borreguero LJ, de la Pompa JL. Mutations in the NOTCH pathway regulator MIB1 cause left ventricular noncompaction cardiomyopathy. *Nat Med* 2013;**19**:193–201.
12. Trembley MA, Velasquez LS, de Mesy Bentley KL, Small EM. Myocardin-related transcription factors control the motility of epicardium-derived cells and the maturation of coronary vessels. *Development* 2015;**142**:21–30.
13. Verdonschot JAJ, Hazebroek MR, Derks KWJ, Barandiaran Aizpurua A, Merken JJ, Wang P, Bierau J, van den Wijngaard A, Schalla SM, Abdul Hamid MA, van Bilsen M, van Empel VPM, Knackstedt C, Brunner-La Rocca HP, Brunner HG, Krapels IPC, Heymans SRB. Titin cardiomyopathy leads to altered mitochondrial energetics, increased fibrosis and long-term life-threatening arrhythmias. *Eur Heart J* 2018;**39**:864–873.
14. Muelas N, Hackman P, Luque H, Garcés-Sánchez M, Azorín I, Suominen T, Sevilla T, Mayordomo F, Gómez L, Martí P, María Millán J, Udd B, Vílchez JJ. MYH7 gene tail mutation causing myopathic profiles beyond Laing distal myopathy. *Neurology* 2010;**75**:732–741.
15. Zhang D, Li Y, Heims-Waldron D, Bezzerides V, Guatimosim S, Guo Y, Gu F, Zhou P, Lin Z, Ma Q, Liu J, Wang DZ, Pu WT. Mitochondrial cardiomyopathy caused by elevated reactive oxygen species and impaired cardiomyocyte proliferation. *Circ Res* 2018;**122**:74–87.
16. Giacomelli E, Bellin M, Sala L, van Meer BJ, Tertoolen LG, Orlova VV, Mummery CL. Three-dimensional cardiac microtissues composed of cardiomyocytes and endothelial cells co-differentiated from human pluripotent stem cells. *Development* 2017;**144**:1008–1017.
17. Wang L, Yu P, Zhou B, Song J, Li Z, Zhang M, Guo G, Wang Y, Chen X, Han L, Hu S. Single-cell reconstruction of the adult human heart during heart failure and recovery reveals the cellular landscape underlying cardiac function. *Nat Cell Biol* 2020;**22**:108–119.
18. Risebro CA, Searles RG, Melville AA, Ehler E, Jina N, Shah S, Pallas J, Hubank M, Dillard M, Harvey NL, Schwartz RJ, Chien KR, Oliver G, Riley PR. Prox1 maintains muscle structure and growth in the developing heart. *Development* 2009;**136**:495–505.
19. Bersell K, Arab S, Haring B, Kuhn B. Neuregulin1/ErbB4 signaling induces cardiomyocyte proliferation and repair of heart injury. *Cell* 2009;**138**:257–270.
20. Paik DT, Chandy M, Wu JC. Patient and disease-specific induced pluripotent stem cells for discovery of personalized cardiovascular drugs and therapeutics. *Pharmacol Rev* 2020;**72**:320–342.
21. Udono T, Takahashi K, Nakayama M, Yoshinoya A, Totsune K, Murakami O, Durlu YK, Tamai M, Shibahara S. Induction of adrenomedullin by hypoxia in cultured retinal pigment epithelial cells. *Invest Ophthalmol Vis Sci* 2001;**42**:1080–1086.
22. Sun Y, Xiong X, Wang X. HIF1alpha/miR-199a/ADM feedback loop modulates the proliferation of human dermal microvascular endothelial cells (HDMECs) under hypoxic condition. *Cell Cycle* 2019;**18**:2998–3009.
23. Botting KJ, McMillen IC, Forbes H, Nyengaard JR, Morrison JL. Chronic hypoxemia in late gestation decreases cardiomyocyte number but does not change expression of hypoxia-responsive genes. *J Am Heart Assoc* 2014;**3**:e000531.
24. Sandireddy R, Cibi DM, Gupta P, Singh A, Tee N, Uemura A, Epstein JA, Singh MK. Semaphorin 3E/PlexinD1 signaling is required for cardiac ventricular compaction. *JCI Insight* 2019;**4**:e125908.
25. Christoffels VM, Keijser AG, Houweling AC, Clout DE, Moorman AF. Patterning the embryonic heart: identification of five mouse Iroquois homeobox genes in the developing heart. *Dev Biol* 2000;**224**:263–274.
26. Wang Y, Toh YC, Li Q, Nugraha B, Zheng B, Lu TB, Gao Y, Ng MM, Yu H. Mechanical compaction directly modulates the dynamics of bile canaliculi formation. *Integr Biol (Camb)* 2013;**5**:390–401.
27. Junatas KL, Tonar Z, Kubikova T, Liska V, Palek R, Mik P, Kralickova M, Witter K. Stereological analysis of size and density of hepatocytes in the porcine liver. *J Anat* 2017;**230**:575–588.
28. Herron TJ, Rocha AM, Campbell KF, Ponce-Balbuena D, Willis BC, Guerrero-Serna G, Liu Q, Klos M, Musa H, Zarzoso M, Bizy A, Furness J, Anumonwo J, Mironov S, Jalife J. Extracellular matrix-mediated maturation of human pluripotent stem cell-derived cardiac monolayer structure and electrophysiological function. *Circ Arrhythm Electrophysiol* 2016;**9**:e003638.
29. Liu Q, Hu T, He L, Huang X, Tian X, Zhang H, He L, Pu W, Zhang L, Sun H, Fang J, Yu Y, Duan S, Hu C, Hui L, Zhang H, Quertermous T, Xu Q, Red-Horse K, Wythe JD, Zhou B. Genetic targeting of sprouting angiogenesis using Apln-CreER. *Nat Commun* 2015;**6**:6020.
30. Wu B, Zhang Z, Lui W, Chen X, Wang Y, Chamberlain AA, Moreno-Rodriguez RA, Markwald RR, O'Rourke BP, Sharp DJ, Zheng D, Lenz J, Baldwin HS, Chang CP, Zhou B. Endocardial cells form the coronary arteries by angiogenesis through myocardial-endocardial VEGF signaling. *Cell* 2012;**151**:1083–1096.
31. Chen HI, Sharma B, Akerberg BN, Numi HJ, Kivela R, Saharinen P, Aghajanian H, McKay AS, Bogard PE, Chang AH, Jacobs AH, Epstein JA, Stankunas K, Alitalo K, Red-Horse K. The sinus venosus contributes to coronary vasculature through VEGFC-stimulated angiogenesis. *Development* 2014;**141**:4500–4512.
32. Paik DT, Cho S, Tian L, Chang HY, Wu JC. Single-cell RNA sequencing in cardiovascular development, disease and medicine. *Nat Rev Cardiol* 2020;**17**:457–473.
33. Myers JC, Dion AS, Abraham V, Amenta PS. Type XV collagen exhibits a widespread distribution in human tissues but a distinct localization in basement membrane zones. *Cell Tissue Res* 1996;**286**:493–505.
34. Tomono Y, Naito I, Ando K, Yonezawa T, Sado Y, Hirakawa S, Arata J, Okigaki T, Ninomiya Y. Epitope-defined monoclonal antibodies against multiplexin collagens demonstrate that type XV and XVIII collagens are expressed in specialized basement membranes. *Cell Struct Funct* 2002;**27**:9–20.
35. Connelly JJ, Cherepanova OA, Doss JF, Karaoli T, Lillard TS, Markunas CA, Nelson S, Wang T, Ellis PD, Langford CF, Haynes C, Seo DM, Goldschmidt-Clermont PJ, Shah SH, Kraus WE, Hauser ER, Gregory SG. Epigenetic regulation of COL15A1 in smooth muscle cell replicative aging and atherosclerosis. *Hum Mol Genet* 2013;**22**:5107–5120.
36. Eklund L, Piuhola J, Komulainen J, Sormunen R, Ongvarrasopone C, Fassler R, Muona A, Ilves M, Ruskoaho H, Takala TE, Pihlajaniemi T. Lack of type XV collagen causes a skeletal myopathy and cardiovascular defects in mice. *Proc Natl Acad Sci U S A* 2001;**98**:1194–1199.
37. Rasi K, Piuhola J, Czabanka M, Sormunen R, Ilves M, Leskinen H, Rysa J, Kerkela R, Janmey P, Heljasvaara R, Peuhkurinen K, Vuolteenaho O, Ruskoaho H, Vajkoczy P, Pihlajaniemi T, Eklund L. Collagen XV is necessary for modeling of the extracellular matrix and its deficiency predisposes to cardiomyopathy. *Circ Res* 2010;**107**:1241–1252.
38. Hurskainen M, Ruggiero F, Hagg P, Pihlajaniemi T, Huhtala P. Recombinant human collagen XV regulates cell adhesion and migration. *J Biol Chem* 2010;**285**:5258–5265.
39. Kim JE, Kim SJ, Lee BH, Park RW, Kim KS, Kim IS. Identification of motifs for cell adhesion within the repeated domains of transforming growth factor-beta-induced gene, betaig-h3. *J Biol Chem* 2000;**275**:30907–30915.
40. Billings PC, Whitbeck JC, Adams CS, Abrams WR, Cohen AJ, Engelsberg BN, Howard PS, Rosenbloom J. The transforming growth factor-beta-inducible matrix protein (beta)ig-h3 interacts with fibronectin. *J Biol Chem* 2002;**277**:28003–28009.
41. Reinboth B, Thomas J, Hanssen E, Gibson MA. Beta ig-h3 interacts directly with biglycan and decorin, promotes collagen VI aggregation, and participates in ternary complexing with these macromolecules. *J Biol Chem* 2006;**281**:7816–7824.
42. Harston RK, Kuppuswamy D. Integrins are the necessary links to hypertrophic growth in cardiomyocytes. *J Signal Transduct* 2011;**2011**:1–8.
43. Israeli-Rosenberg S, Manso AM, Okada H, Ross RS. Integrins and integrin-associated proteins in the cardiac myocyte. *Circ Res* 2014;**114**:572–586.

44. Lemke SB, Schnorrer F. Mechanical forces during muscle development. *Mech Dev* 2017;**144**:92–101.
45. Baxter RC, Firth SM. Modulation of human IGF binding protein-3 activity by structural modification. *Prog Growth Factor Res* 1995;**6**:215–222.
46. Li P, Cavallero S, Gu Y, Chen TH, Hughes J, Hassan AB, Bruning JC, Pashmforoush M, Sucov HM. IGF signaling directs ventricular cardiomyocyte proliferation during embryonic heart development. *Development* 2011;**138**:1795–1805.
47. Lee SH, Takahashi M, Honke K, Miyoshi E, Osumi D, Sakiyama H, Ekuni A, Wang X, Inoue S, Gu J, Kadomatsu K, Taniguchi N. Loss of core fucosylation of low-density lipoprotein receptor-related protein-1 impairs its function, leading to the upregulation of serum levels of insulin-like growth factor-binding protein 3 in Fut8-/- mice. *J Biochem* 2006;**139**:391–398.
48. Grkovic S, O'Reilly VC, Han S, Hong M, Baxter RC, Firth SM. IGFBP-3 binds GRP78, stimulates autophagy and promotes the survival of breast cancer cells exposed to adverse microenvironments. *Oncogene* 2013;**32**:2412–2420.
49. Der SD, Zhou A, Williams BR, Silverman RH. Identification of genes differentially regulated by interferon alpha, beta, or gamma using oligonucleotide arrays. *Proc Natl Acad Sci U S A* 1998;**95**:15623–15628.
50. Loeb KR, Haas AL. The interferon-inducible 15-kDa ubiquitin homolog conjugates to intracellular proteins. *J Biol Chem* 1992;**267**:7806–7813.
51. Zhao C, Denison C, Huibregtse JM, Gygi S, Krug RM. Human ISG15 conjugation targets both IFN-induced and constitutively expressed proteins functioning in diverse cellular pathways. *Proc Natl Acad Sci U S A* 2005;**102**:10200–10205.
52. Yu SL, Chan PK, Wong CK, Szeto CC, Ho SC, So K, Yu MM, Yim SF, Cheung TH, Wong MC, Cheung JL, Yeung AC, Li EK, Tam LS. Antagonist-mediated down-regulation of Toll-like receptors increases the prevalence of human papillomavirus infection in systemic lupus erythematosus. *Arthritis Res Ther* 2012;**14**:R80.
53. Wong HK, Cheung TT, Cheung BM. Adrenomedullin and cardiovascular diseases. *JRSM Cardiovasc Dis* 2012;**1**:1–7.
54. Mishima K, Kato J, Kuwasako K, Ito K, Imamura T, Kitamura K, Eto T. Effects of endothelin on adrenomedullin secretion and expression of adrenomedullin receptors in rat cardiomyocytes. *Biochem Biophys Res Commun* 2001;**287**:264–269.
55. Autelitano DJ, Ridings R. Adrenomedullin signalling in cardiomyocytes is dependent upon CRLR and RAMP2 expression. *Peptides* 2001;**22**:1851–1857.

Translational Perspective

Left ventricular non-compaction (LVNC) is a disease characterized by the inability of the myocardium to compact, severely affecting heart function and leading to mortality. The aetiology is poorly understood, but knowledge regarding the pathophysiology could lead to novel therapeutic interventions. Evidence suggests that defects in vascular endothelium/endocardium can contribute to LVNC development. Using a mouse model, we identify proteins expressed in vascular cells that induce cardiomyocyte responses that cause non-compaction. We also identify a protein expressed in normal endothelial cells that has the opposite effect. These studies can inspire development of clinical strategies aimed at understanding and treating non-compaction cardiomyopathy.